Food Packaging and Shelf Life 26 (2020) 100575

Contents lists available at ScienceDirect

Food Packaging and Shelf Life

journal homepage: www.elsevier.com/locate/fpsl

Dextran-coated silver nanoparticles for improved barrier and controlled antimicrobial properties of nanocellulose films used in food packaging

Vesna Lazić [a], Vera Vivod [b], Zdenka Peršin [b], Milovan Stoiljković [a], Ishara S. Ratnayake [c], Phillip S. Ahrenkiel [c], Jovan M. Nedeljković [a], Vanja Kokol [b,*]

[a] Vinča Institute of Nuclear Sciences, University of Belgrade, P.O. Box 522, Belgrade, Serbia
[b] University of Maribor, Faculty of Mechanical Engineering, Institute of Engineering Materials and Design, Slovenia
[c] South Dakota School of Mines and Technology, 501 E. Saint Joseph Street, Rapid City, SD 57701, USA

ARTICLE INFO

Keywords:
Nanocellulose
Dextran-coated silver nanoparticles
Barrier properties
Antimicrobial activity
Food packaging

ABSTRACT

The effect of dextran-coated silver nanoparticles (Ag NPs 12.0 ± 1.9 nm) loading (0–0.42 wt%) on the mechanical, barrier, and antimicrobial properties of thin (50–60 μm) films prepared from cellulose nanofibrils by solvent casting method were studied as eco-friendly and food-preservative packaging materials. The presence of dextran was shown to act not only as a dispersing media for Ag NPs and controlling its release but also as a moisture-resistant sealable additive that, synergetically with reduced oxygen permeability, may preserve the food against bacteria growth. Thus, significantly reduced Oxygen Transmission Rates (from 2.07 to 1.40-0.78 $cm^3\ m^{-2}d^{-1}$) and hydrophilicity (from 20.8° to 52.4° for MilliQ water, and from 35-37° to 62-74° for 3 % acetic acid and 0.9 % NaCl simulant solutions), yielding a 99.9 % inhibition of *Escherichia coli* after five repeated cycles of 24 h exposure to 0.9 % NaCl solution was displayed, supported by a controlled release of Ag^+ ions (below the toxicologically harmful threshold, <0.5 mg L^{-1}).

1. Introduction

Nanocellulose is being studied increasingly for its application in bio-based food packaging materials, acting as a coating or an inter-layer film, which is related to its low-cost, renewability, biodegradability, non-toxicity, as well as high barrier property for gases, and, above all, an excellent oxygen barrier permeation (Belbekhouche et al., 2011; Fukuya, Senoo, Kotera, Yoshimoto, & Sakata, 2014; Minelli et al., 2010; Shanmugam, Doosthosseini, Varanasi, Garnier, & Batchelor, 2019), that may change food's chemical, physical, and microbiological properties (Aulin, Gallstedt, & Lindström, 2010; Barhoum, Samyn, Ohlund, & Dufresne, 2017; El-Wakil, Hassan, Abou-Zeid, & Dufresne, 2015; Hubbe et al., 2017). In addition, to control the undesirable growth of foodborne pathogens and, by this, to extend the shelf life of products, maintaining their safety and quality, new nanocellulose structured materials combined with various metallic (Cu (Jia, Mei, Cheng, Zhou, & Zhang, 2012), Ag (Ahamed, Alsalhi, & Siddiqui, 2010; Ilić et al., 2009; Vukoje, Lazić et al., 2014; Xu, Li, Yue, & Lu, 2017; Zhou, Kong, Kundu, Cirillo, & Liang, 2012), Au (Daniel & Astruc, 2004; Zhou et al., 2012)) and metal-oxide nanoparticles (CuO (Carpenter et al., 2015; Yoosefi Booshehri, Wang, & Xu, 2015), TiO_2 (Mihailović et al., 2011), ZnO (Lefatshe, Muiva, & Kebaabetswe, 2017; Zhao, Guo, Hu, Guo, & Pan, 2018), MnO_2 (Wang et al., 2016), deposited on a surface or loaded/-blended into/within the nanocellulose/biopolymer network, have been exploited to improve the properties of food packaging materials.

Silver nanoparticles (Ag NPs) are the most used antimicrobial substance among metallic nanoparticles (Duncan, 2011) due to the broad-spectrum of their antibacterial activities (Pal, Tak, & Song, 2007; Panacek et al., 2006; Pirtarighat, Ghannadnia, & Baghshahi, 2019; Radetić et al., 2008; Rai, Yadav, & Gade, 2009), and profitable capacities such as stability and relatively low toxicity to eukaryotic cells (Fortunati et al., 2014). Their proficient antimicrobial performance is related to extremely small particle size, resulting in cell penetration (Cho et al., 2018; Daniel & Astruc, 2004; Morones et al., 2005), the interaction of released Ag^+ ions with amino and carboxyl groups of peptidoglycan contained in the cell walls (Lok et al., 2007; Vazquez-Muñoz et al., 2017), and generation of oxidative stress that affect the replication of DNA or the collapse of the proton-motive force across the cytoplasmic membrane (Holt & Bard, 2005; Marini et al., 2007; Xiu, Ma, & Alvarez, 2011). However, as the overuse of Ag NPs raises some health

* Corresponding author.
E-mail address: vanja.kokol@um.si (V. Kokol).

https://doi.org/10.1016/j.fpsl.2020.100575
Received 21 April 2020; Received in revised form 21 August 2020; Accepted 25 September 2020
Available online 18 October 2020

and ecological concerns (Kittler, Greulich, Diendorf, Köller, & Epple, 2010) due to a cumulative increase in the concentration of released Ag^+ ions (Ahamed et al., 2010; Marambio-Jones & Hoek, 2010), phytochemicals, having a dual role as reducing and capping agents, have been used for their preparation (Ahmed, Ahmad, Swami, & Ikram, 2016; Davidović et al., 2017; Rajan, Chandran, Harper, Yun, & Kalaichelvan, 2015; Rolim et al., 2019; Song & Kim, 2008) to overcome these issues. In this frame, Ag NPs have been immobilized onto the amino-functionalized (Guo, Filpponen, Su, Laine, & Rojas, 2016) or carboxylated (Marrez, Abdelhamid, & Darwesh, 2019; Shin, Gwon, Lee, & Yoo, 2018) cellulose nanofibrils (CNFs) via electrostatic interactions, or Au NPs have been synthesized in situ on CNFs (Van Rie & Thielemans, 2017) providing slow and concentration controlled release kinetics of ions to minimize their toxicity potential. In addition, Ag NPs have been prepared by simple one-pot synthetic route and "green synthesis" approach using plant extracts or products of bacterial metabolite (Davidović et al., 2017) to act as both reducing and capping agents.

The purpose of the present study was to define the effect of colloidal dextran-coated Ag NPs on the morpho-structural, mechanical, oxygen barrier, and wetting properties of CNF-based hybrid films, prepared by the solvent casting method. It was hypothesized that dextran acts not only as capping molecules for Ag NPs, but also as an oxygen adsorber and moisture-resistant additive, which is, to the best of our knowledge, the first such study. Besides, to gain a better insight into the limitations of prepared hybrid films for practical use, the release kinetics of Ag^+ ions were investigated thoroughly using 0.9 % NaCl as a test liquid, acting as a food stimulant. The concentration-dependent antibacterial activities of so prepared films were analyzed against Gram-negative *Escherichia coli* and Gram-positive *Staphylococcus aureus* under long-run-working conditions in five repeated cycles.

2. Experimental

2.1. Preparation of dextran-coated Ag NPs and CNF-based hybrid films

Cellulose nanofibrils (CNFs) with diameters in the range of 10−70 nm and lengths on the micrometer scale, having chain-like structures, were purchased from the University of Maine in the USA. Dextran was synthesized from bacteria *Leuconostoc mesenteroides* T3, isolated from kefir grain at the Faculty of Technology and Metallurgy, University of Belgrade (Davidovic, Miljkovic, Antonovic, Rajilic-Stojanovic, & Dimitrijevic-Brankovic, 2015; Davidović et al., 2015). All other chemicals were purchased from Sigma Aldrich and used as received.

The colloids, consisting of dextran-coated Ag NPs, were prepared following the procedure described in the literature (Davidović et al., 2017). Briefly, silver colloids were synthesized by adding 3.4 mg of $AgNO_3$ into 100 mL of 0.03 % dextran solution at pH 9 and 60 °C. The solution was stirred vigorously for 3 h. The appearance of a yellow-brown color indicated the formation of metallic Ag NPs.

The Ag-CNF films were prepared by mixing 2 mL of CNF suspension (3.0 wt.-%) and 2 mL of silver colloids having three different concentrations, followed by the addition of MilliQ water up to the final volume of 57.6 mL. Then, the resulting mixtures were cast on 110 mm in diameter Petri-dishes and air-dried at room temperature to form water-stable films by slow evaporation of the solvent. In parallel, two blank films were prepared, one from CNFs and the second with the addition of dextran. The pristine (0.5 wt.-%) CNFs film and the CNFs film with 0.005 wt.-% of dextran were labeled as 0 and 0-dex, respectively. The nanocomposite films with incorporated dextran-coated Ag NPs into the (0.5 wt.-%) CNFs matrix were labeled as 1-dex, 2-dex, and 3-dex, reflecting the ascending concentration of Ag, which was found to be 0.12 ± 0.01, 0.21 ± 0.02, and 0.41 ± 0.02 wt.-%, respectively, and corresponding dextran addition (0.0025, 0.005 and 0.01 wt.-%).

2.2. Characterization of the films

Structural characterization of the films and distribution of Ag NPs was performed on a Transmission Electron Microscope (TEM) JEOL JEM-2100 LaB_6. For that purpose, films were embedded in an epoxy resin (Epofix, Electron Microscopy Sciences) and cured overnight at 40 °C. Samples were then microtomed at room temperature to a thickness of around 70 nm, using an RMC PowerTome-XL ultramicrotome and Diatome diamond knife with a water-filled boat. The microtomed sections were transferred from the water surface to copper grids using a Perfect Loop. Also, Scanning Electron Microscopy (SEM) analysis of the films was performed by using a low-vacuum microscope (FEI Quanta 200 3D, Wien, Austria) to characterize the morphology of the samples.

Film thickness was measured with the electronic digital caliper and inputted to the computer program WinPerme OX2-230 W3-330(En). The measurements were performed at three different places to obtain average values.

The absorption spectra of silver colloids were measured using a Thermo Scientific Evolution 600 UV/Vis spectrophotometer. The optical properties of Ag-CNF films were studied by diffuse reflectance spectroscopy (Shimadzu UV–vis UV-2600 spectrophotometer equipped with an integrated sphere ISR-2600 Plus).

The content of silver in the Ag-CNF nanocomposite films was determined using Inductively Coupled Plasma Optic Emission Spectroscopy (ICP-OES Thermo Scientific iCAP 7400). Before the measurements, all samples were digested in a Milestone Start D microwave using concentrated HNO_3 and H_2O_2. The release of Ag^+ ions from Ag-CNF films was studied at static conditions for a long period (3 weeks) at room temperature. The Ag-CNF films (0.1 g) were placed into flasks containing 100 mL of saline solution (0.9 % NaCl). Sampling (5 mL aliquot) was performed at the desired incubation period, and the concentration of the released Ag^+ ions was measured by the ICP-OES technique. The obtained results are presented in the form of the average values of three measurements. It is important to point out that, due to the high concentration ratio between Cl^- ions from saline and released Ag^+ ions, the AgBr does not precipitate, but the formation of the Ag-Br complexes takes place.

The Oxygen Transmission Rate (OTR) of the films were determined according to ISO 15105-2/ASTM D3985 standard at 23 ± 0.5 °C and Relative Humidity/RH of 50 ± 1.5 % by using an Oxygen Transmission Rate test machine Perme OX2/230 (Labthink Instruments Co., Ltd.). The samples were conditioned for 24 h before measurements. Flat film samples were clamped into the diffusion cell, which was purged of residual oxygen using an oxygen-free carrier gas. Then pure oxygen (99.9 %) was introduced into the outside chamber of the diffusion cell (50 ± 1.5 % RH) and the oxygen molecules permeating through the film to the inside chamber were conveyed to the coulometric sensor by the carrier gas (N_2). The OTR was calculated by normalizing the flow rate at a steady-state with respect to the oxygen pressure gradient and expressed in (mL m^{-2} day^{-1}). Three independent determinations were carried out for each film sample, and the mean of these three values is given as the final result.

Contact Angle (CA) measurements of the films were performed using an OCA20 Contact Angle measurement system from Dataphysics (Germany). All measurements were conducted at room temperature on both sides of the films, using a 3 mL volume of test liquids. MilliQ-water, 50 % ethanol-water (EtOH), 3 % acetic acid (CH_3COOH) and 0.9 % sodium chloride (NaCl) solutions were used as test liquids, acting as food stimulants according to the Commission Regulation 2016/1416 of 24 August 2016, amending and correcting Regulation (EU) No 10/2011 on plastic materials and articles intended to come into contact with food. The pendant drop analysis (using the Young-Laplace equation) was also performed to measure the surface tension (γ) of the test liquids. The three-phase contact line of a liquid drop, formed on the surface, was analyzed. The equilibrium angle was established by a balance of surface tension parallel to the liquid-solid interface. The CA of the tested liquid

on the sample surface was evaluated using the Young-Laplace equation. Each CA value was the average of at least six drops of liquid per surface, where at least three measurements were made for each side of the film.

The tensile strength at maximum tensile strain upon breaking was measured using a Shimadzu AGS-X electromechanical universal testing machine. The samples were cut into a vessel shape according to Standard ISO 6892-1:2010-method B, and attached to clamps at a distance of 30.8 mm, and tested at a speed of 0.05 mm s^{-1} and room temperature. At least three measurements were performed for each film, and the mean value is given as the final result.

2.3. Antimicrobial ability of films

The time-dependent antimicrobial ability of Ag-CNF films was evaluated against Gram-negative bacteria *E. coli* (ATCC 25922) and Gram-positive bacteria *S. aureus* (ATCC 25923). Briefly, the quantitative antimicrobial test was performed as follows: 10 mg pieces of film samples were placed in 10 mL saline solution (0.9 % NaCl) containing ~10^5–10^6 CFU mL^{-1} of the tested bacteria and incubated at 37 °C. The 0.1 mL aliquots were taken after 2, 7, 12, and 24 h to determine the number of viable cells after 24 h of growing in tryptone soy agar. The percentage of Reduction (R %) was calculated according to Eq. (1):

$$R(\%) = 100 \times (C_0 - C)/C_0 \quad (1)$$

where C_0 is the number (CFU mL^{-1}) of microorganisms in the control film (pristine CNFs), and C is the number (CFU mL^{-1}) of microorganisms in the Ag-CNF nanocomposite films.

Also, the time-dependent antibacterial activities of Ag-CNF nanocomposite films *E. coli* were tested under long-run conditions in five repeated cycles using a concentration of 1.0 mg mL^{-1} of the nanocomposite. After 24 h of contact between bacterial species and the film, the sample was separated by sterile tweezers and moved into 10 mL of saline solution containing ~10^5–10^6 CFU mL^{-1} of the bacteria for a new cycle. The determination of viable bacterial cells is described in the previous paragraph.

3. Results and discussion

3.1. Structural and morphological characterization of dextran-coated Ag NPs and corresponding CNF-based hybrid films

A typical TEM image and corresponding Selected Area Electron Diffraction (SAED) pattern of synthesized colloidal Ag particles are presented in Fig. 1A and B, respectively. The presence of nearly spherical Ag particles with narrow size distribution can be noticed. Their average size, determined from the statistical sample of over two hundred particles, was found to be 12.0 ± 1.9 nm. Analysis of the SAED pattern revealed diffraction rings that belong to the (111), (200), (220), and (311) planes from the face-centered cubic phase of the silver.

The SEM and TEM images of the Ag-CNF film with the lowest content of Ag NPs (sample 1-dex) are shown in Fig. 1C and D, respectively. It is clear that, upon incorporation, the non-agglomerated dextran-coated Ag NPs are distributed randomly in a dense and uniform network of CNFs. The images of films with a higher content of Ag NPs (samples 2-dex and 3-dex; Supplementary Information (Fig. S1) are similar to the presented one.

The Kubelka-Munk transformations of reflection data for pristine CNFs film, CNFs film containing dextran, and hybrid Ag-CNF films are shown in Fig. 2. The surface plasmon resonance bands of Ag NPs incorporated in CNF films resemble the shape of the free-standing Ag

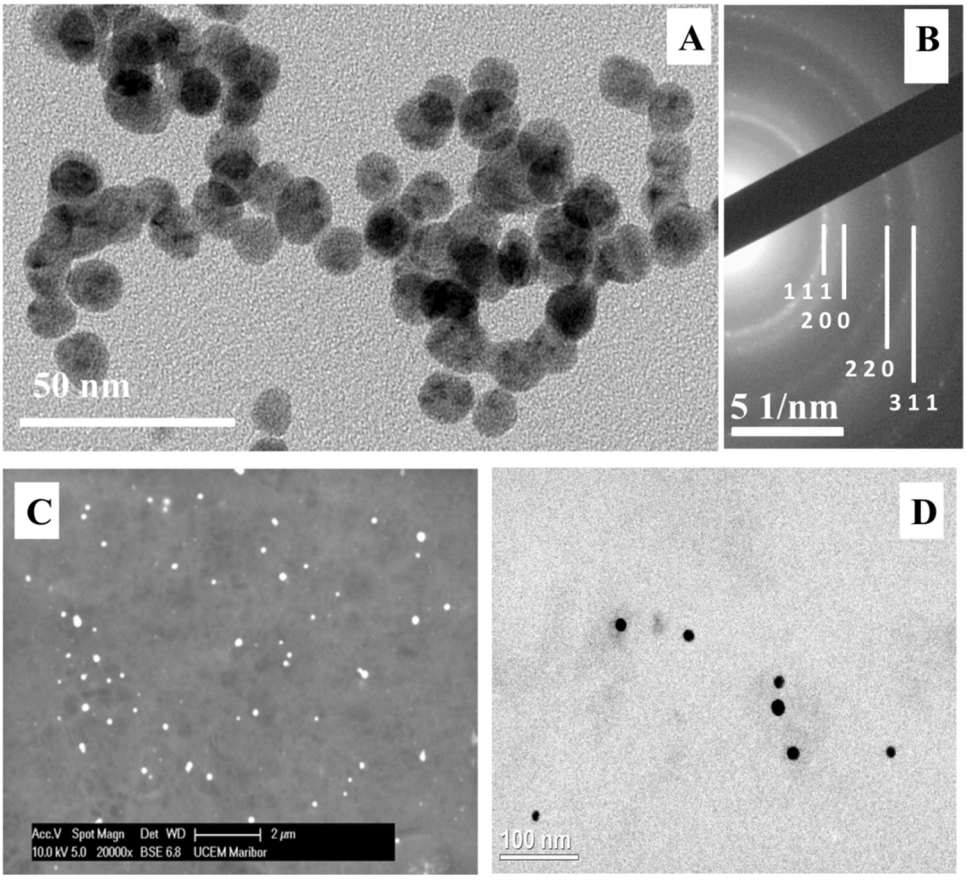

Fig. 1. Low-magnification TEM image of dextran-coated Ag NPs **(A)** with corresponding SAED pattern **(B)**, and typical **(C)** SEM and TEM **(D)** images of hybrid film with the lowest content of Ag NPs (0.12 wt.-%).

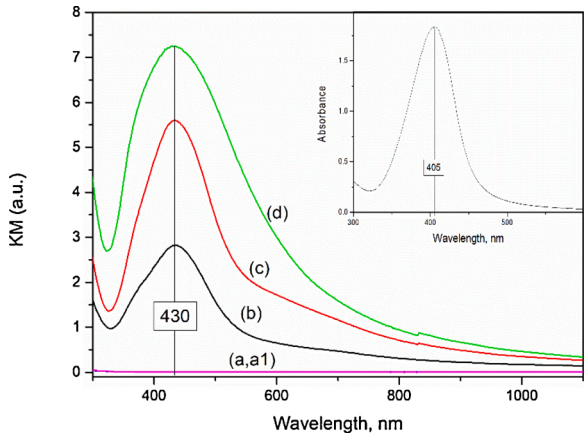

Fig. 2. Kubelka-Munk transformations of diffuse reflection data of pristine CNFs films prepared without (a) and with dextran (a1), as well as hybrid films with various content of dextran-coated Ag NPs: (b) 1-dex, (c) 2-dex, (d) 3-dex; inset: absorption spectrum of pristine 2×10^{-4} M Ag colloid used for the preparation of the films.

NPs (see inset). The surface plasmon resonance band peaking at 405 nm indicates that the colloid consists of nanometer-sized Ag particles. Thus, the absorption spectrum is consistent with the TEM analysis. The red-shift of the peak maxima (~430 nm) in hybrid films is a consequence of the larger values of refraction indexes of nano-cellulose and dextran (1.499 and 1.380, respectively) (Landry, Alemdar, & Blanchet, 2011) than that of water (1.333).

3.2. Mechanical properties of the films

The mechanical properties of hybrid Ag-CNF and reference films are presented in Table 1. The addition of dextran to CNFs film (0-dex) did not change Young's modulus significantly (from 2.7 to 2.3 GPa) but had a positive effect on the strength by reaching the maximum value among all the samples (105 MPa) while reducing its elongation at break (from 5.5 to 2.5 %).

On the other side, when comparing the pristine CNFs film (0-dex) with those containing dextran-coated Ag NPs (1-dex to 3-dex), an increase of the maximum strength was observed with the increase of the content of silver, reaching the highest value (94 MPa), similar to the pristine film (0), for the sample with the highest content of dextran-coated Ag NPs (3-dex). However, the differences in mechanical properties for all these films are small, within experimental errors. The Young's modulus also increased compared to both reference films but remained comparable for all dextran-coated Ag NPs containing films (4.1–4.5 GPa).

To conclude, the addition of dextran-coated Ag NPs improved the mechanical properties of the films, mainly due to the presence of dextran. By being a complex branched glucan consisting of glucose molecules, dextran increases H-bonding and stacking interactions between the cellulose fibrils (Müller-Dethlefs & Hobza, 2000), thus acting as a reinforcement and compatibilized compound. A similar effect was reported by other research groups using different polysaccharide molecules, such as sorbitol (Herrera, Mathew, & Oksman, 2017), starch, and sucrose (Balakrishnan et al., 2019) as an additive to cellulose films.

Table 1
Tensile Strength (TS), Young's modulus (EM), and Elongation At Break (EAB) for pristine CNFs films without (0) and with dextran (0-dex), and hybrid films with various content of dextran-coated Ag NPs (1-dex, 2-dex, 3-dex).

Sample	TS (MPa)	EM (GPa)	EAB (%)
0	92 ± 7	2.7 ± 0.6	5.5 ± 0.1
0-dex	105 ± 7	2.3 ± 0.9	2.5 ± 0.3
1-dex	79 ± 23	4.1 ± 0.9	2.6 ± 0.7
2-dex	86 ± 24	4.3 ± 0.6	2.7 ± 0.6
3-dex	94 ± 23	4.5 ± 0.9	2.9 ± 0.6

All values are obtained from six independent measurements; standard deviation values are included.

3.3. Oxygen barrier properties of the films

The permeability of oxygen (OTR) in hybrid films as a function of the content of dextran-coated Ag NPs, and the permeability in the reference films, was monitored at standard conditions, i.e., at a temperature of 23 ± 0.5 °C and RH of 50 ± 1.5 %). The graph presenting the OTR values over the time of measurement, i.e., until the flow rate is normalizing, is presented in Fig. 3, and corresponding data collected in the inserted Table.

The OTR value, required for most food products, should lie between 0.1–30 $cm^3\ m^{-2}\ d^{-1}$, depending on the oxygen sensitivity of the food type, although the material is considered as a "high oxygen barrier" if its OTR value is even less than 30 $cm^3\ m^{-2}\ d^{-1}$. The OTR values of materials govern two principal factors, the thickness and the polymer chemistry. The latter one dictates the diffusivity and solubility, and, hence, the permeability of the penetrant solvent molecules through a dense polymer matrix. However, the film thickness is unimportant, if acting as an additional layer in multi-layer packagings, like ours, and it was not considered, although it is generally accepted, the thicker the film, the better the oxygen barrier. The addition of dextran to CNF (samples 0 and 0-dex) reduced the film's thickness from about 53 to 49 μm, while the incorporation of dextran-coated Ag NPs leads to their increase to about 60 μm.

The films prepared from hydrophilic polymers such as cellulose, at low RH, display high barriers against oxygen due to the large amount of −OH groups in their structure. Oxygen has a low polarity, and, consequently, a weak interaction with the highly polar −OH groups from cellulose. The increase of RH induces the interaction of the −OH groups with the highly polar water molecules, weakening the hydrogen bonds that hold the polymer chains together, and acting as a plasticizer that swells their native structure. Consequently, oxygen permeability is influenced by the presence of water molecules (Aulin et al., 2010; Auras, Harte, & Selke, 2004; Balakrishnan et al., 2019; Belbekhouche et al., 2011; Lagarón, Giménez, Gavara, & Saura, 2001), and, thus, increasing the OTR values (Tammelin & Vartiainen). Therefore, to present the effect of the film's nanostructure on the OTR values, measurements have been carried out over the time until the flow rate is normalized, as shown in Fig. 3.

The addition of dextran into the CNF matrix film (0-dex) leads to a denser and tightly packed thin-layer film structure (49 μm), but also the highest OTR values of about 2.07 $cm^3\ m^{-2}\ d^{-1}$, which is stabilized after 15 days. The OTR values of films containing dextran-coated Ag NPs (from 1-dex to 3-dex) are reducing significantly faster to constant values (after 3–10 days), despite the presence of dextran. Most likely, Ag NPs are blocking the majority of −OH groups from dextran, and, consequently, they are not available for interaction with those from CNFs. Because of that, the diffusion path for molecular permeation through the films is increased (Tammelin & Vartiainen), diminishing oxygen transport through such a matrix.

Obviously, decrease of the OTR values with an increase of the content of the dextran-coated Ag NPs can be observed when values are stabilized (Fig. 3, inserted Table). The OTR value of sample 3-dex (0.78 $cm^3\ m^{-2}\ d^{-1}$) with the highest content of Ag NPs (0.41 wt.-%) is almost three times smaller than the OTR value for pristine CNFs film (2.07 $cm^3\ m^{-2}\ d^{-1}$). This value is similar, or even better, compared to the OTR values reported in the literature for CNF-based and other biopolymer-based films, prepared, for example, from PET or PS (Aulin et al., 2010; Balakrishnan et al., 2019; Fukuzumi et al., 2011; Fukuzumi, Saito, Iwata, Kumamoto, & Isogai, 2009; Herrera et al., 2017; Wu, Huang, Li, Xiao, & Wang, 2018).

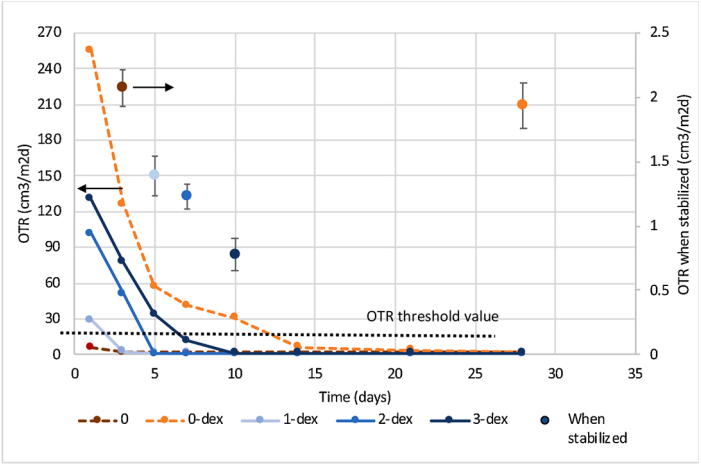

Sample	Content of Ag (wt.-%)	Content of Dex (wt.-%)	Thickness of film (μm)	OTR when stabilized ($cm^3\ m^{-2}\ d^{-1}$)
0	0	0	53.2±1.5	2.07 ±0.15
0-dex	0	0.0050	49.0±1.0	1.93±0.18
1-dex	0.12±0.01	0.0025	60.3±7.1	1.40 ±0.16
2-dex	0.21±0.02	0.0050	59.0±3.4	1.23 ±0.10
3-dex	0.41±0.02	0.0100	61.0±6.2	0.78 ±0.13

Fig. 3. Composition, thickness, and Oxygen Transmission Rate (OTR) values for pristine CNFs (0.5 wt.-%) films without (0) and with dextran (0-dex), as well as hybrid films with various content of dextran-coated Ag NPs (1-dex, 2-dex, 3-dex) as a function of time until the OTR values are stabilized (T = 23 ± 0.5 °C, RH = 50 ± 1.5 %); the final values are provided in inserted Table.

3.4. Hydrophilic nature and wetting properties of the films

The development of nanomaterials for food contact packaging is accompanied by safety concerns, related to the transfer of nanomaterials from the packaging film to the food (Störmer, Bott, Kemmer, & Franz, 2017). Ag NPs easily oxidize to ions, but, in a slightly reductive environment, can precipitate again, mimicking migration. On the other hand, Ag NPs can be detached from the dextran, and further from CNFs` surfaces, due to the weak binding, influencing the physicomechanical properties of nanocomposite films, such as surface energy and wettability. Also, this process is highly dependent on the environmental conditions, above all, the presence of moisture.

The macroscopic Contact Angle (CA) measurements of the reference and hybrid CNF films with different contents of dextran-coated AgNPs were, thus, performed, to determine the wetting behavior of prepared samples in physical contact with various liquids (MilliQ water, as well as 50 % Et-OH, 3 % acetic acid, and 0.9 % NaCl solutions), representing general (acidic) food stimulants (Regulation, 2016). The CA measurements can also provide information about the moisture sensitivity and sealability of the films, which govern barrier behavior towards water (Nair, Zhu, Deng, & Ragauskas, 2014; Wang et al., 2018), as well as the chemical composition and topology (surface roughness and heterogeneity) of their surface (Andresen, Johansson, Tanem, & Stenius, 2006; Belbekhouche et al., 2011; Wu, Saito, Yang, Fukuzumi, & Isogai, 2014), which, altogether also govern the adhesion of bacteria (Teno, González-Gaitano, & González-Benito, 2017). In general, smoother surfaces have higher CA than rough ones, although rough surfaces can also have high CA, due to the heterogeneous wetting related to the formation of air compartments between droplets and the surface.

Some general features can be discerned based on the results presented in Table 2. First, a noticeable increase of CA values can be observed upon the incorporation of dextran-coated Ag NPs into the CNFs matrix for all studied liquids. This effect is rather the consequence of the simultaneous increase of dextran concentration than Ag NPs themselves since CA values are much higher for reference films containing dextran (0-dex) independently of the used solvent. The CA values of hybrid CNF films (1-dex to 3-dex) for MilliQ water with the highest surface tension

Table 2
Contact Angle (°) values of various liquids (MilliQ water, 50 % Et-OH, 3 % CH_3COOH, and 0.9 % NaCl) for pristine CNFs films without (0) and with dextran (0-dex), and hybrid films with various content of dextran-coated Ag NPs (1-dex, 2-dex, 3-dex); values of Surface Tension (γ), density (ρ), and viscosity (η) of liquids used in the evaluation of CA are also provided.

Sample	MilliQ water γ = 72.8 mN m^{-1} ρ = 1.010 g cm^{-3} η = 1.002 mPas	50 % Et-OH γ = 28.6 mN m^{-1} ρ = 0.915 g cm^{-3} η = 2.68 mPas	3 % CH_3COOH γ = 64.5 mN m^{-1} ρ = 1.002 g cm^{-3} η = 1.223 mPas	0.9 % NaCl γ = 65.35 mN m^{-1} ρ = 1.063 g cm^{-3} η = 1.168 mPas
0	20.8 ± 3.5	17.5 ± 4.5	35.5 ± 4.7	37.1 ± 4.8
0-dex	66.9 ± 4.6	35.5 ± 4.0	n.d.	59.0 ± 5.8
1-dex	28.8 ± 4.2	16.0 ± 2.0	39.2 ± 4.8	53.6 ± 4.9
2-dex	44.5 ± 4.7	18.9 ± 4.9	53.7 ± 3.7	65.7 ± 3.7
3-dex	52.4 ± 3.0	19.7 ± 3.5	62.3 ± 5.0	74.8 ± 4.8

All values are obtained from six independent measurements; standard deviation values are included.

(~72 mN m^{-1}) were thus increased from 20.8° (for pristine CNF film without dextran, 0) to the range of 28.8–52.4°, which is similar to recently published data by Thiagamani et al. (Thiagamani et al., 2019). The same behavior was observed for other liquids with similar surface tensions (~65 mN m^{-1}); an increase of CA upon the incorporation of dextran-coated Ag NPs from about 35.5 and 37.1° to about 62.3 and 74.6° for 3 % CH_3COOH and 0.9 % NaCl, respectively. It can be concluded that the relatively lower CA values may be a consequence of the presence of free −OH groups on the external surfaces (Hubbe, Gardner, & Shen, 2015; Orsuwan, Shankar, Wang, Sothornvit, & Rhim, 2016) on one side, and surface tension of the liquid on the other. Since the incorporated dextran-coated Ag NPs are primarily attracted by the polar −OH groups from dextran molecules, which are, further, also interacting with the −OH groups of CNFs, as already discussed above, the reduction of their availability is most likely the reason for the increased CA values of hybrid films. Also, CA values are strongly dependent on the surface tension of the applied liquids. Generally, the

addition of inorganic salts increases the surface tension of water (Boström, Williams, & Ninham, 2001; Matubayasi, Takayama, Ito, & Takata, 2011), while the addition of organic substances has the opposite effect. That is indeed the case for 50 % EtOH and 3 % acetic acid, with surface tension values of 28.6 and 64.5 mN m^{-1}, respectively. On the other hand, the surface tension of a salt-solution (0.9 % NaCl) is smaller (65.35 mN m^{-1}) compared to MilliQ water (72.8 mN m^{-1}), which, according to Boström, et al. (Boström et al., 2001), could be a consequence of the attractive interaction between Na^+ and water molecules that keep the Na^+ ions at the air-water interface. Also, Sghaier et al. (Sghaier, Prat, & Ben Nasrallah, 2006) proved that the CA increases with an increase of NaCl concentration on all tested hydrophilic surfaces. Our results exhibited the same trend. CA values for 0.9 % NaCl solution are higher compared to the corresponding CA values for MilliQ water for both reference CNFs film, as well as hybrid Ag-CNF films, except for the CNFs film containing the only dextran, which may indicate a reduction in the hydrophilic nature and associated wetting properties in these films.

3.5. Antimicrobial properties of the films and the release of Ag^+ ions into food-stimulant liquids

The time-dependent antimicrobial ability of hybrid CNF-based films was tested against Gram-negative bacteria *E. coli* and Gram-positive bacteria *S. aureus*. The antibacterial tests were carried out with two concentrations of hybrid films (1.0 and 2.0 mg mL^{-1} using 0.9 % NaCl solution as an incubation media). The data concerning the counted number of viable cells and the percentage of microbial reductions with a lower concentration of hybrid films are collected in Table 3, while the data for the higher concentration are shown in Supporting Information 1. All hybrid films, after 24 h in contact with *E. coli,* induced the complete reduction of viable cells (99.9 %). The influence of the Ag content in the hybrid films on the antibacterial performance against *E. coli* is observable at the shorter time of contact. For example, after 7 h, the reduction of *E. coli* cells was around 77 % for a lower Ag concentration (1-dex film), while, for the higher concentration, the reduction reached satisfactory values (>96 %) (Supporting Information 1). The obtained results are in agreement with recent studies reporting the high antibacterial activity against *E. coli* for nanocomposites consisting of polyvinyl alcohol, nanocellulose, starch-capped Ag NPs, glycerine (Sarwar, Niazi, Jahan, Ahmad, & Hussain, 2018), as well as porous hybrids consisting of bacterial nanocellulose and Ag NPs (Berndt, Wesarg, Wiegand, Kralisch, & Müller, 2013). On the other hand, the antibacterial test against the Gram-positive bacteria *S. aureus* indicated negligible antimicrobial activity of such hybrid films (Supporting Information 1), which may be due to the release of the relatively low amount of Ag^+ ions, as well as a thicker cell wall and different membrane structure of this type of bacteria (Sarwar et al., 2018). Lower antimicrobial efficiency against *S. aureus* compared to *E. coli* has also been observed for Ag NPs attached to macroporous polymer support (Vukoje et al., 2017; Vukoje, Džunuzović, Dimitrijević, Phillip Ahrenkiel, & Nedeljković, 2019; Vukoje, Džunuzović et al., 2014), as well as inorganic supports such as hydroxyapatite (Lazić et al., 2018), and magnetite (Lazić et al., 2019).

The long-term antibacterial performance of all hybrid films against *E. coli* was studied in five repeated cycles. The films' concentration was kept constant in all experiments (1 mg mL^{-1}), while the frequency of sampling was 24 h. To avoid the accumulation of released Ag^+ ions, that can give false results, before each new cycle, the hybrid films were separated from the solution, and a new portion of live bacterial cells (~10^5 CFU mL^{-1}) was introduced. The obtained results are presented in Table 4. The complete reduction of viable *E. coli* cells was observed for all investigated film samples with different content of Ag NPs, the antibacterial performance of which was preserved during a period of five days, i.e., under long-run working conditions. The antibacterial efficiency of dextran-coated and in CNF matrix incorporated Ag NPs is comparable to the performance of similar in size Ag NPs deposited onto inorganic supports (Lazić et al., 2018, 2019), which might be associated with the films` low wetting ability.

The cumulative release of Ag^+ ions from the Ag-CNF films was analyzed further by placing them into the 0.9 % NaCl solution over a period of three weeks. Kinetic data concerning the release of Ag^+ ions are presented in Fig. 4. Several features are recognizable from the obtained data. First, after 500 h, the cumulative concentration of Ag^+ ions in the surrounding media was smaller than 0.5 mg L^{-1} for all hybrid films (Fig. 4A), which is significantly below the ecologically harmful concentration (1.0 mg L^{-1}) (Panacek et al., 2006). Second, the initial rates of dissolution of incorporated Ag NPs were quite similar for all hybrid films, as well as the saturation concentrations. Most likely, this is a consequence of the small differences in the silver content among prepared samples. Third, the percentage of released Ag^+ ions (Fig. 4B) was nearly proportional to the initial concentration ratio of metallic silver in the hybrids. It should be noticed that, after three weeks, the percentage of dissolved Ag NPs did not exceed 10 % for the hybrid sample with the highest content of Ag NPs. Almost the same percentage of dissolved Ag NPs from nanocellulose composite films with grape seed extracts and immobilized Ag NPs was reported (Wu, Deng, Luo, & Deng,

Table 4
The antibacterial ability of hybrid films (1 mg mL^{-1}) against *E. coli* after 24 h of sampling in five repeated cycles.

		Hybrid films with various content of Ag		
Cycle	Inoculum (CFU mL^{-1})	1-dex (0.12 wt.-%)	2-dex (0.21 wt.-%)	3-dex(0.41 wt.-%)
I	4.0×10^5	<10	<10	<10
II	2.0×10^5	<10	<10	<10
III	1.4×10^5	<10	<10	<10
IV	6.0×10^5	75	<10	<10
V	2.0×10^5	5×10^2	<10	<10

Table 3
The antibacterial ability of hybrid films (1 mg mL^{-1}) with various content of Ag (1-dex: 0.12 wt.-%, 2-dex: 0.21 wt.-%, 3-dex: 0.41 wt.-%), against *E. coli* as a function of time (*E. coli* inoculum 1.7×10^6 CFU mL^{-1} in 0.9 % NaCl solution).

Sample	TIME (h)								
	2			7			24		
	CFU mL^{-1}	R(%)	R_{av}*(%)	CFU mL^{-1}	R(%)	R_{av}*(%)	CFU mL^{-1}	R(%)	R_{av}*(%)
	7.2×10^5	57.6		4.5×10^5	73.5		0	99.9	
1-dex	7.9×10^5	53.5	58.4 ± 4.4	5.0×10^5	70.6	77.2 ± 7.4	100	99.9	99.9
	6.1×10^5	64.1		2.1×10^5	87.6		0	99.9	
	7.2×10^5	57.6		4.2×10^5	75.3		0	99.9	
2-dex	4.5×10^5	73.5	68.8 ± 7.9	3.8×10^5	77.6	76.3 ± 1.0	10	99.9	99.9
	4.2×10^5	75.3		4.1×10^5	75.9		0	99.9	
	5.8×10^5	65.9		4.1×10^5	75.9		0	99.9	
3-dex	4.5×10^5	73.5	60.2 ± 13.8	3.9×10^5	77.1	77.3 ± 1.0	0	99.9	99.9
	1.0×10^6	41.2		3.6×10^5	78.8		0	99.9	

* All Rav values are obtained from three independent measurements; standard deviation values are included.

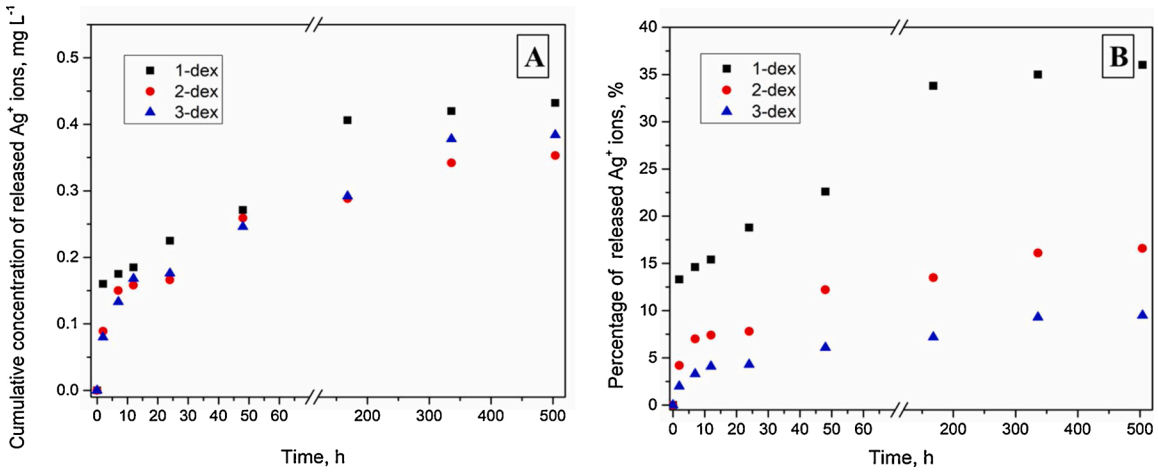

Fig. 4. (A) Cumulative concentration of released Ag^+ ions from hybrid films with various content of dextran-coated Ag NPs (1-dex, 2-dex, 3-dex) as a function of time. (B) The percentage of released Ag^+ ions normalised to the content of Ag NPs in the films as a function of time. A 0.9 % NaCl solution was used for this study.

2019). Shin et al. analyzed the release of Ag^+ ions from nanocellulose fibers with Ag NPs, and they got a releasing rate approximately 10 times higher than in our system (Shin et al., 2018).

4. Conclusion

Dextran-coated Ag NPs are used as a compatibilized, barrier, and antibacterial colloidal additive to the CNF matrix, in the form of a thin-layer film, to improve its performance in biodegradable and eco-friendly food packaging applications. A controllable release of Ag^+ ions with an antimicrobial performance under long-run (three-weeks) food simulation working conditions was established, being attributed to a reduction in the hydrophilic nature and associated wetting properties of the films containing dextran-coated Ag NPs, and being supported with significant suppression of the permeation of oxygen, which highlighted their potential as food preservatives against bacterial growth. Such films also display an improved Young's modulus without altering their tensile strength and have preserved their flexibility. These results indicate that such hybrid films might serve as a sustainable and end-of-life disposal replacement for their synthetic counterparts in food-contact or multi-layer food packaging applications.

CRediT authorship contribution statement

Vesna Lazić: Formal analysis, Investigation, Visualization. **Vera Vivod:** Formal analysis, Investigation. **Zdenka Peršin:** Formal analysis, Investigation, Data curation. **Milovan Stoiljković:** Formal analysis, Investigation. **Ishara S. Ratnayake:** Formal analysis, Investigation. **Phillip S. Ahrenkiel:** Formal analysis, Investigation. **Jovan M. Nedeljković:** Conceptualization, Supervision, Writing - review & editing. **Vanja Kokol:** Methodology, Writing - original draft, Supervision.

Acknowledgments

This study was carried out within the Bilateral project between the Republic of Slovenia and the Republic of Serbia (No. 44). The Serbian team was supported by the Ministry of Education, Science and Technological Development of the Republic of Serbia. The Slovenian team was supported by the Slovenian Research Agency (Research Programme P2-0118). South Dakota participants were supported by the State of South Dakota and the National Science Foundation-EPSCoR of the United States (Award IIA-1355423).

Appendix A. Supplementary data

Supplementary material related to this article can be found, in the online version, at doi:https://doi.org/10.1016/j.fpsl.2020.100575.

References

Ahamed, M., Alsalhi, M. S., & Siddiqui, M. K. (2010). Silver nanoparticle applications and human health. *Clinica Chimica Acta, 411*(23–24), 1841–1848.
Ahmed, S., Ahmad, M., Swami, B. L., & Ikram, S. (2016). A review on plants extract mediated synthesis of silver nanoparticles for antimicrobial applications: A green expertise. *Journal of Advanced Research, 7*(1), 17–28.
Andresen, M., Johansson, L.-S., Tanem, B. S., & Stenius, P. (2006). Properties and characterization of hydrophobized microfibrillated cellulose. *Cellulose, 13*(6), 665–677.
Aulin, C., Gallstedt, M., & Lindström, T. (2010). Oxygen and oil barrier properties of microfibrillated cellulose films and coatings. *Cellulose (London), 17*(3), 559–574.
Auras, R., Harte, B., & Selke, S. (2004). Effect of water on the oxygen barrier properties of poly(ethylene terephthalate) and polylactide films. *Journal of Applied Polymer Science, 92*(3), 1790–1803.
Balakrishnan, P., Sreekala, M. S., Geethamma, V. G., Kalarikkal, N., Kokol, V., Volova, T., & Thomas, S. (2019). Physicochemical, mechanical, barrier and antibacterial properties of starch nanocomposites crosslinked with pre-oxidised sucrose. *Industrial Crops and Products, 130*, 398–408.
Barhoum, A., Samyn, P., Ohlund, T., & Dufresne, A. (2017). Review of recent research on flexible multifunctional nanopapers. *Nanoscale, 9*(40), 15181–15205.
Belbekhouche, S., Bras, J., Siqueira, G., Chappey, C., Lebrun, L., Khelifi, B., & Dufresne, A. (2011). Water sorption behavior and gas barrier properties of cellulose whiskers and microfibrils films. *Carbohydrate Polymers, 83*(4), 1740–1748.
Berndt, S., Wesarg, F., Wiegand, C., Kralisch, D., & Müller, F. A. (2013). Antimicrobial porous hybrids consisting of bacterial nanocellulose and silver nanoparticles. *Cellulose, 20*(2), 771–783.
Boström, M., Williams, D. R. M., & Ninham, B. W. (2001). Surface tension of electrolytes: Specific ion effects explained by dispersion forces. *Langmuir, 17*(15), 4475–4478.
Carpenter, B. L., Scholle, F., Sadeghifar, H., Francis, A. J., Boltersdorf, J., Weare, W. W., … Ghiladi, R. A. (2015). Synthesis, characterization, and antimicrobial efficacy of photomicrobicidal cellulose paper. *Biomacromolecules, 16*(8), 2482–2492.
Cho, Y.-M., Mizuta, Y., Akagi, J.-I., Toyoda, T., Sone, M., & Ogawa, K. (2018). Size-dependent acute toxicity of silver nanoparticles in mice. *Journal of Toxicologic Pathology, 31*(1), 73–80.
Daniel, M. C., & Astruc, D. (2004). Gold nanoparticles: Assembly, supramolecular chemistry, quantum-size-related properties, and applications toward biology, catalysis, and nanotechnology. *Chemical Reviews, 104*(1), 293–346.
Davidovic, S., Miljkovic, M., Antonovic, D., Rajilic-Stojanovic, M., & Dimitrijevic-Brankovic, S. (2015). Water Kefir grain as a source of potent dextran producing lactic acid bacteria. *Hemijska Industrija, 69*(6), 595–604.
Davidović, S., Miljković, M., Lazić, V., Jović, D., Jokić, B., Dimitrijević, S., … Radetić, M. (2015). Impregnation of cotton fabric with silver nanoparticles synthesized by dextran isolated from bacterial species Leuconostoc mesenteroides T3. *Carbohydrate Polymers, 131*, 331–336.
Davidović, S., Lazić, V., Vukoje, I., Papan, J., Anhrenkiel, S. P., Dimitrijević, S., & Nedeljković, J. M. (2017). Dextran coated silver nanoparticles—Chemical sensor for selective cysteine detection. *Colloids and Surfaces B: Biointerfaces, 160*, 184–191.
Duncan, T. V. (2011). Applications of nanotechnology in food packaging and food safety: Barrier materials, antimicrobials and sensors. *Journal of Colloid and Interface Science, 363*(1), 1–24.

El-Wakil, N. A., Hassan, E. A., Abou-Zeid, R. E., & Dufresne, A. (2015). Development of wheat gluten/nanocellulose/titanium dioxide nanocomposites for active food packaging. *Carbohydrate Polymers, 124*, 337–346.
Fortunati, E., Rinaldi, S., Peltzer, M., Bloise, N., Visai, L., Armentano, I., & Kenny, J. M. (2014). Nano-biocomposite films with modified cellulose nanocrystals and synthesized silver nanoparticles. *Carbohydrate Polymers, 101*, 1122–1133.
Fukuya, M. N., Senoo, K., Kotera, M., Yoshimoto, M., & Sakata, O. (2014). Enhanced oxygen barrier property of poly(ethylene oxide) films crystallite-oriented by adding cellulose single nanofibers. *Polymer, 55*(22), 5843–5846.
Fukuzumi, H., Saito, T., Iwata, T., Kumamoto, Y., & Isogai, A. (2009). Transparent and high gas barrier films of cellulose nanofibers prepared by TEMPO-mediated oxidation. *Biomacromolecules, 10*(1), 162–165.
Fukuzumi, H., Saito, T., Iwamoto, S., Kumamoto, Y., Ohdaira, T., Suzuki, R., … Isogai, A. (2011). Pore size determination of TEMPO-oxidized cellulose nanofibril films by positron annihilation lifetime spectroscopy. *Biomacromolecules, 12*(11), 4057–4062.
Guo, J., Filpponen, I., Su, P., Laine, J., & Rojas, O. J. (2016). Attachment of gold nanoparticles on cellulose nanofibrils via click reactions and electrostatic interactions. *Cellulose, 23*(5), 3065–3075.
Herrera, M. A., Mathew, A. P., & Oksman, K. (2017). Barrier and mechanical properties of plasticized and cross-linked nanocellulose coatings for paper packaging applications. *Cellulose, 24*(9), 3969–3980.
Holt, K. B., & Bard, A. J. (2005). Interaction of silver(I) ions with the respiratory chain of Escherichia coli: An electrochemical and scanning electrochemical microscopy study of the antimicrobial mechanism of micromolar Ag+. *Biochemistry, 44*(39), 13214–13223.
Hubbe, M. A., Gardner, D. J., & Shen, W. (2015). Contact angles and wettability of cellulosic surfaces: A review of proposed mechanisms and test strategies. *BioResources, 10*(4) (2015).
Hubbe, M. A., Ferrer, A., Tyagi, P., Yin, Y., Salas, C., Pal, L., … Rojas, O. J. (2017). Nanocellulose in thin films, coatings, and plies for packaging applications: A review. *BioResources, 12*(1) (2017).
Ilić, V., Šaponjić, Z., Vodnik, V., Potkonjak, B., Jovančić, P., Nedeljković, J., … Radetić, M. (2009). The influence of silver content on antimicrobial activity and color of cotton fabrics functionalized with Ag nanoparticles. *Carbohydrate Polymers, 78*(3), 564–569.
Jia, B., Mei, Y., Cheng, L., Zhou, J., & Zhang, L. (2012). Preparation of copper nanoparticles coated cellulose films with antibacterial properties through one-step reduction. *ACS Applied Materials & Interfaces, 4*(6), 2897–2902.
Kittler, S., Greulich, C., Diendorf, J., Köller, M., & Epple, M. (2010). Toxicity of silver nanoparticles increases during storage because of slow dissolution under release of silver ions. *Chemistry of Materials, 22*(16), 4548–4554.
Lagarón, J. M., Giménez, E., Gavara, R., & Saura, J. J. (2001). Study of the influence of water sorption in pure components and binary blends of high barrier ethylene–vinyl alcohol copolymer and amorphous polyamide and nylon-containing ionomer. *Polymer, 42*(23), 9531–9540.
Landry, V., Alemdar, A., & Blanchet, P. (2011). Nanocrystalline cellulose: Morphological, physical, and mechanical properties. *Forest Products Journal, 61*(2), 104–112.
Lazić, V., Smičiklas, I., Marković, J., Lončarević, D., Dostanić, J., Ahrenkiel, S. P., … Nedeljković, J. M. (2018). Antibacterial ability of supported silver nanoparticles by functionalized hydroxyapatite with 5-aminosalicylic acid. *Vacuum, 148*, 62–68.
Lazić, V., Mihajlovski, K., Mraković, A., Illés, E., Stoiljković, M., Ahrenkiel, S. P., … Nedeljković, J. M. (2019). Antimicrobial activity of silver nanoparticles supported by magnetite. *ChemistrySelect, 4*(14), 4018–4024.
Lefatshe, K., Muiva, C. M., & Kebaabetswe, L. P. (2017). Extraction of nanocellulose and in-situ casting of ZnO/cellulose nanocomposite with enhanced photocatalytic and antibacterial activity. *Carbohydrate Polymers, 164*, 301–308.
Lok, C., N, Ho, C., M, Chen, R., He, Q., … Che, C. M. (2007). Silver nanoparticles: partial oxidation and antibacterial activities. *Journal of Biological Inorganic Chemistry, 12*(4), 527–534.
Marambio-Jones, C., & Hoek, E. M. V. (2010). A review of the antibacterial effects of silver nanomaterials and potential implications for human health and the environment. *Journal of Nanoparticle Research, 12*(5), 1531–1551.
Marini, M., De Niederhausern, S., Iseppi, R., Bondi, M., Sabia, C., Toselli, M., … Pilati, F. (2007). Antibacterial activity of plastics coated with silver-doped organic-inorganic hybrid coatings prepared by sol-gel processes. *Biomacromolecules, 8*, 1246–1254.
Marrez, D. A., Abdelhamid, A. E., & Darwesh, O. M. (2019). Eco-friendly cellulose acetate green synthesized silver nano-composite as antibacterial packaging system for food safety. *Food Packaging and Shelf Life, 20*, Article 100302.
Matubayasi, N., Takayama, K., Ito, R., & Takata, R. (2011). Thermodynamic quantities of surface formation of aqueous electrolyte solutions X. Aqueous solution of 2:1 valence-type salts. *Journal of Colloid and Interface Science, 356*(2), 713–717.
Mihailović, D., Šaponjić, Z., Radoičić, M., Lazović, S., Baily, C., J, … Radetić, M. (2011). Functionalization of cotton fabrics with corona/air RF plasma and colloidal TiO2 nanoparticles. *Cellulose, 18*(3), 811–825.
Minelli, M., Baschetti, M. G., Doghieri, F., Ankerfors, M., Lindström, T., Siró, I., … Plackett, D. (2010). Investigation of mass transport properties of microfibrillated cellulose (MFC) films. *Journal of Membrane Science, 358*(1), 67–75.
Morones, J. R., Elechiguerra, J. L., Camacho, A., Holt, K., Kouri, J. B., Ramirez, J. T., … Yacaman, M. J. (2005). The bactericidal effect of silver nanoparticles. *Nanotechnology, 16*(10), 2346–2353.
Müller-Dethlefs, K., & Hobza, P. (2000). Noncovalent interactions: A challenge for experiment and theory. *Chemical Reviews, 100*(1), 143–168.
Nair, S. S., Zhu, J. Y., Deng, Y., & Ragauskas, A. J. (2014). High performance green barriers based on nanocellulose. *Sustainable Chemical Processes, 2*(1), 23.
Orsuwan, A., Shankar, S., Wang, L.-F., Sothornvit, R., & Rhim, J.-W. (2016). Preparation of antimicrobial agar/banana powder blend films reinforced with silver nanoparticles. *Food Hydrocolloids, 60*(Supplement C), 476–485.
Pal, S., Tak, Y. K., & Song, J. M. (2007). Does the antibacterial activity of silver nanoparticles depend on the shape of the nanoparticle? A study of the Gram-negative bacterium Escherichia coli. *Applied and Environmental Microbiology, 73*(6), 1712–1720.
Panacek, A., Kvitek, L., Prucek, R., Kolar, M., Vecerova, R., Pizurova, N., … Zboril, R. (2006). Silver colloid nanoparticles: synthesis, characterization, and their antibacterial activity. *The Journal of Physical Chemistry B, 110*(33), 16248–16253.
Pirtarighat, S., Ghannadnia, M., & Baghshahi, S. (2019). Green synthesis of silver nanoparticles using the plant extract of Salvia spinosa grown in vitro and their antibacterial activity assessment. *Journal of Nanostructure in Chemistry, 9*(1), 1–9.
Radetić, M., Ilić, V., Vodnik, V., Dimitrijević, S., Jovančić, P., Šaponjić, Z., … Nedeljković, J. M. (2008). Antibacterial effect of silver nanoparticles deposited on corona-treated polyester and polyamide fabrics. *Polymers for Advanced Technologies, 19*(12), 1816–1821.
Rai, M., Yadav, A., & Gade, A. (2009). Silver nanoparticles as a new generation of antimicrobials. *Biotechnology Advances, 27*(1), 76–83.
Rajan, R., Chandran, K., Harper, S. L., Yun, S.-I., & Kalaichelvan, P. T. (2015). Plant extract synthesized silver nanoparticles: An ongoing source of novel biocompatible materials. *Industrial Crops and Products, 70*, 356–373.
Regulation, C. (2016). In C. Regulation (Ed.), *Amending and correcting regulation (EU) No 10/2011 on plastic materials and articles intended to come into contact with food* (Vol. 2016/1416 of 24 August 2016).
Rolim, W. R., Pelegrino, M. T., de Araújo Lima, B., Ferraz, L. S., Costa, F. N., Bernardes, J. S., … Seabra, A. B. (2019). Green tea extract mediated biogenic synthesis of silver nanoparticles: Characterization, cytotoxicity evaluation and antibacterial activity. *Applied Surface Science, 463*, 66–74.
Sarwar, M. S., Niazi, M. B. K., Jahan, Z., Ahmad, T., & Hussain, A. (2018). Preparation and characterization of PVA/nanocellulose/Ag nanocomposite films for antimicrobial food packaging. *Carbohydrate Polymers, 184*, 453–464.
Sghaier, N., Prat, M., & Ben Nasrallah, S. (2006). On the influence of sodium chloride concentration on equilibrium contact angle. *Chemical Engineering Journal, 122*(1), 47–53.
Shanmugam, K., Doosthosseini, H., Varanasi, S., Garnier, G., & Batchelor, W. (2019). Nanocellulose films as air and water vapour barriers: A recyclable and biodegradable alternative to polyolefin packaging. *Sustainable Materials and Technologies, 22*, Article e00115.
Shin, J. U., Gwon, J., Lee, S. Y., & Yoo, H. S. (2018). Silver-incorporated nanocellulose fibers for antibacterial hydrogels. *ACS Omega, 3*(11), 16150–16157.
Song, J. Y., & Kim, B. S. (2008). Rapid biological synthesis of silver nanoparticles using plant leaf extracts. *Bioprocess and Biosystems Engineering, 32*(1), 79.
Störmer, A., Bott, J., Kemmer, D., & Franz, R. (2017). Critical review of the migration potential of nanoparticles in food contact plastics. *Trends in Food Science & Technology, 63*, 39–50.
Tammelin, T., & Vartiainen, J. Nanocellulose Films and Barriers. Handbook of Green Materials. 2014 (pp. 213–229).
Teno, J., González-Gaitano, G., & González-Benito, J. (2017). Poly (ethylene-co-vinyl acetate) films prepared by solution blow spinning: Surface characterization and its relation with E. coli adhesion. *Polymer Testing, 60*, 140–148.
Thiagamani, S. M. K., Rajini, N., Siengchin, S., Varada Rajulu, A., Hariram, N., & Ayrilmis, N. (2019). Influence of silver nanoparticles on the mechanical, thermal and antimicrobial properties of cellulose-based hybrid nanocomposites. *Composites Part B: Engineering, 165*, 516–525.
Van Rie, J., & Thielemans, W. (2017). Cellulose–gold nanoparticle hybrid materials. *Nanoscale, 9*(25), 8525–8554.
Vazquez-Muñoz, R., Borrego, B., Juárez-Moreno, K., García-García, M., Mota Morales, J. D., Bogdanchikova, N., … Huerta-Saquero, A. (2017). Toxicity of silver nanoparticles in biological systems: Does the complexity of biological systems matter? *Toxicology Letters, 276*, 11–20.
Vukoje, I. D., Džunuzović, E. S., Lončarević, D. R., Dimitrijević, S., Ahrenkiel, S. P., & Nedeljković, J. M. (2017). Synthesis, characterization, and antimicrobial activity of silver nanoparticles on poly(GMA-co-EGDMA) polymer support. *Polymer Composites, 38*(6), 1206–1214.
Vukoje, I. D., Džunuzović, E. S., Dimitrijević, S., Phillip Ahrenkiel, S., & Nedeljković, J. M. (2019). Size-dependent antibacterial properties of Ag nanoparticles supported by amino-functionalized poly(GMA-co-EGDMA) polymer. *Polymer Composites, 40*(7), 2901–2907.
Vukoje, I. D., Džunuzović, E. S., Vodnik, V. V., Dimitrijević, S., Ahrenkiel, S. P., & Nedeljković, J. M. (2014). Synthesis, characterization, and antimicrobial activity of poly(GMA-co-EGDMA) polymer decorated with silver nanoparticles. *Journal of Materials Science, 49*(19), 6838–6844.
Vukoje, I., Lazić, V., Vodnik, V., Mitrić, M., Jokić, B., Phillip Ahrenkiel, S., … Radetić, M. (2014). The influence of triangular silver nanoplates on antimicrobial activity and color of cotton fabrics pretreated with chitosan. *Journal of Materials Science, 49*(13), 4453–4460.
Wang, L., He, H., Zhang, C., Sun, L., Liu, S., & Wang, S. (2016). Antimicrobial activity of silver loaded MnO2 nanomaterials with different crystal phases against Escherichia coli. *Journal of the Environmental Sciences, 41*, 112–120.
Wang, J., Gardner, D. J., Stark, N. M., Bousfield, D. W., Tajvidi, M., & Cai, Z. (2018). Moisture and oxygen barrier properties of cellulose nanomaterial-based films. *ACS Sustainable Chemistry & Engineering, 6*(1), 49–70.
Wu, C.-N., Saito, T., Yang, Q., Fukuzumi, H., & Isogai, A. (2014). Increase in the water contact angle of composite film surfaces caused by the assembly of hydrophilic

nanocellulose fibrils and nanoclay platelets. *ACS Applied Materials & Interfaces, 6* (15), 12707–12712.
Wu, Z., Huang, X., Li, Y. C., Xiao, H., & Wang, X. (2018). Novel chitosan films with laponite immobilized Ag nanoparticles for active food packaging. *Carbohydrate Polymers, 199*, 210–218.
Wu, Z., Deng, W., Luo, J., & Deng, D. (2019). Multifunctional nano-cellulose composite films with grape seed extracts and immobilized silver nanoparticles. *Carbohydrate Polymers, 205*, 447–455.
Xiu, Z.-M., Ma, J., & Alvarez, P. J. J. (2011). Differential effect of common ligands and molecular oxygen on antimicrobial activity of silver nanoparticles versus silver ions. *Environmental Science & Technology, 45*(20), 9003–9008.
Xu, Y., Li, S., Yue, X., & Lu, W. (2017). Review of silver nanoparticles (AgNPs)-cellulose antibacterial composites. *BioResources, 13*(1) (2018).
Yoosefi Booshehri, A., Wang, R., & Xu, R. (2015). Simple method of deposition of CuO nanoparticles on a cellulose paper and its antibacterial activity. *Chemical Engineering Journal, 262*, 999–1008.
Zhao, S.-W., Guo, C.-R., Hu, Y.-Z., Guo, Y.-R., & Pan, Q.-J. (2018). The preparation and antibacterial activity of cellulose/ZnO composite: A review. *Open Chemistry, 16*, 9.
Zhou, Y., Kong, Y., Kundu, S., Cirillo, J. D., & Liang, H. (2012). Antibacterial activities of gold and silver nanoparticles against Escherichia coli and bacillus Calmette-Guerin. *Journal of Nanobiotechnology, 10*, 19.